# CHAPTER 2

# THEORY AND LITERATURE REVIEW

## 2.1 Theoretical considerations

Colorimetry is the branch of color science concerned with specifying numerically the color of a physically defined visual stimulus in such a manner that: (a) when viewed by an observer with normal color vision, under the same observing conditions, stimuli with the same specification look alike, (i.e., are in complete color-match), (b) stimuli that look alike have the same specification and (c) the numbers comprising the specification are continuous functions of the physical parameters defining the spectral radiant power distribution of the stimulus.

The experimental laws of color matching as summed up in an empirical generalization, which we will refer to as the trichromatic generalization, provide the foundation for any system of colorimetry meeting these requirements. The concepts and terms currently employed in colorimetry are, in fact, to a large extent bound up with the trichromatic generalization.

Colorimetry is also concerned with the specification of small color differences that an observer may perceive when the differences in the spectral radiant power distributions of the given visual stimuli are such that a complete color match is not observed. For this purpose, color-difference formulae are used, which in current colorimetric practice are derived from a variety of different blocks of experimental data.*[1]*

The CIE Colorimetric System comprises the essential standards and procedures of measurement that are necessary to make colorimetry a useful tool in science and technology. Their descriptions are not depend on any device; thus it's called device independent color space. It could be treated as Non-uniform and Uniform of perceptual colorimetric system. The non-uniform of perceptual colorimetric system, such as *CIEXYZ* and its linear transforms, is built on a spectroscopic foundation together with the human color matching ability which the psychophysical experiments have shown that the human eye's sensitivity to light's scale is not linear.

To remedy this, the CIE proposed two pseudo uniform colorimetric systems, which denoted as *CIELUV* and *CIELAB*. They are the nonlinear transformation of *CIEXYZ* color space. Therefore, their distance, in space, represents the difference of color perception and simply calculated as Euclidean distance in *CIELAB* space.*[2]*

Another type of color space is device color space, which respect to the nature of each kind of device. Such as the *CMY* color space defines colors within a unit cube by the subtractive color-mixing model. This model provides color stimuli for which the radiant power in the spectra are selectively absorbed by an object such that the remaining spectral radiant power is reflected or transmitted, then received by observer or measuring devices.*[3]*

Color imaging device is a device that used to transform color from one source to other in color imaging system such as system of acquisition, display, and hardcopy. CIE Color spaces are the color spaces that show the ability of human perception.*[4]* Hence it is used to be the reference color space for communication, or transformation,

between any of color imaging device to keep the consistency of device color rendering.*[5]*

To obtain the consistent color imaging system, it's necessary to characterize each device. The characterization of a color output device such as a digital color printer defines the relationship between the device color space and a reference color space. This relationship defines a forward printer model. Several approaches to printer modeling may be divided into two main groups: (a) Physical models, such models are based on knowledge of the physical or chemical behavior of the printing system, and are thus inherently dependent on the technology used (ink jet, dye-sublimation, etc.). An important example of physical models for halftone devices is the *Neugebauer* model, which treats the printed color as an additive mixture of the tristimulus values of the paper, the primary colors, and any overlap of primary colors. (b) Empirical models, such models do not explicitly require knowledge of the physical properties of the printer as they rely only on the measurement of a large number of color samples, used either to optimize a set of linear equations based on regression algorithms, or to build look-up table for 3D interpolation.*[6]*

### 2.1.1 Uniform color spaces and color differences

The *CIELUV* space was often used for describing colors in displays, while *CIELAB* was initially designed for reflective media. Now *CIELAB* is used for most applications and has been chosen as standard colour space for several fields. In this research, the *CIELAB* space is used to be the evaluation of an error of color transformation.

The *CIELAB* pseudo-uniform colour space is defined by the quantities $L*$, $a*$, $b*$ define as:

$$L* = 116 f(Y/Y_n) - 16$$

$$a* = 500[f(X/X_n) - f(Y/Y_n)]$$

$$b* = 200[f(Y/Y_n) - f(Z/Z_n)]$$

where;

$$f(t) = t^{1/3} \qquad\qquad 1 \geq t > 0.008856$$
$$= 7.787t + (16/116) \qquad 0 \leq t \leq 0.008856$$

*(2-1)*

The tristimulus values $X_n$, $Y_n$ and $Z_n$ are those of the nominally white stimulus. $L*$ represents the *lightness* of a color, known as the *CIE 1976* psychometric lightness. The scale of $L*$ is 0 to 100, 0 being the ideal black, and 100 being the reference white. The chromatic of a color can be represented in a two-dimensional $a*$, $b*$ diagram. The $a*$, $b*$ chroma diagram, however, is *not* a chromaticity diagram.

When comparing two colors, specified by *[L₁\*,a₁\*,b₁\*]* with *[L₂\*,a₂\*,b₂\*]*, one widely used measure of the color difference is the *CIE 1976 CIELAB color-difference* which is simply calculated as the *Euclidean* distance in *CIELAB* space, as follows:

$$\Delta E_i = \left\| (\Delta L_i)^2 + (\Delta a_i)^2 + (\Delta b_i)^2 \right\|^{1/2} \qquad (2\text{-}2)$$

The interpretation of $\Delta E_{ab}$ color differences is not straightforward, though. It is commonly stated that the *JND, Just noticeable of difference*, is equal to 1.

A rule of thumb for the practical interpretation of $\Delta E_{ab}$ when two colors are shown side by side is presented as: hardly perceptible for $\Delta E_{ab} < 3$, for $3 < \Delta E_{ab} < 6$ perceptible but acceptable , for $\Delta E_{ab} > 6$ not acceptable.

Another interpretation of $\Delta E_{ab}$ errors for the evaluation of scanners is proposed by *Abrardo*. They classify mean errors of 0-1 as *limit of perception*, 1-3 as *very good quality*, 3-6 as *good quality*, 6-10 as *sufficient*, and more than 10 as *insufficient*. It is noted that the disagreement between these classifications, underlining the fact that the evaluation of quality and acceptability is highly subjective and depends on the application.*[7]*

## 2.1.2 sRGB color space

The dichotomy between the device dependent (e.g. amounts of ink expressed in *CMYK* or digitized video voltages expressed in *RGB*) and device independent colour spaces (such as *CIELAB* or *CIEXYZ*) has created a performance burden on applications that have attempted to avoid device colour spaces. This is primarily due to the complexity of the colour transforms they need to perform to return the colors to device dependent colour spaces. This situation is worsened by a reliability gap between the complexity and variety of the transforms, making it hard to ensure that the system is properly configured. This standard addresses these concerns, serves the needs of PC and Web based colour imaging systems is based on the average

performance of personal computer displays. This solution is supported by the following observations:

- Most computer displays are similar in their key colour characteristics such as the phosphor chromaticities (primaries) and transfer function

- *RGB* spaces are native to displays, scanners and digital cameras, which are the devices with the highest performance constraints

- *RGB* spaces can be made device independent in a straightforward way. They can also describe colour gamut that are large enough for all but a small number of applications.

This combination of factors makes a colorimetric *RGB* space well suited for wide adoption since it can both describe the colors in an unambiguous way and be the native space for actual hardware devices. The new combination is so called as *sRGB* color space.*[8]*

*2.1.3 Regression Analysis*

The polynomial regression is based on the assumption that the correlation between color spaces can be approximated by a set of simultaneous equations. The schematic diagram of the regression method is depicted in Figure 2.1. Sample points in the source color space are selected and their color specifications in the destination space are measured. An equation is chosen for linking the source and destination color specifications.
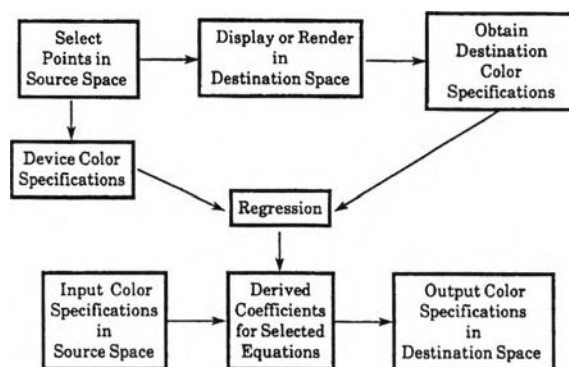
**Figure 2-1** Schematic diagram of the regression method

A regression is performed to select points with known color specifications in both source and destination spaces for deriving the coefficients of the polynomial. The only requirement is that the number of points should be higher than the number of polynomial terms; otherwise, there will be no unique solutions to the simultaneous equations because there are more unknown variables than equations. Using derived coefficients, one can plug the source specifications into the simultaneous equations to compute the destination specifications

The polynomial regression is an application of the multiple linear regression of $m$ variables, where $m$ is a number greater than the number of independent variables. The general approach of the linear regression with $m$ variables is given as follows:

$$P_i = a_1 v_{i1} + a_2 v_{i2} + \ldots\ldots\ldots\ldots + a_m v_{im} \tag{2-3}$$

For the application to the polynomial regression with three independent variables $x$, $y$, and z: $v_1 = x$, $v_2 = y$, and $v_3 = z$. we then set

$v_4 = xy$, $v_5 = yz$, $v_6 = zx$, $v_7 = x^2$, $v_8 = y^2$, $v_9 = z^2$, *etc.*

The coefficients are obtained by

$$a = (V\ V')^{-1}(VP) \qquad\qquad (2\text{-}4)$$

With n sets of inputs, $V$ is a matrix of size $m$ x $n$, where $m$ is the number of terms in the polynomial. $V'$ is the transpose of $V$ that is obtained by interchanging the rows and columns of the matrix $V$, therefore, a matrix of size $n$ x $m$. The product of $VV'$ is an $n$ x $m$ symmetric matrix.

Color transformation by using this method is a relatively simple method compare to many method such as 3D look-up table, the sample points need not be uniformly spaced. The conversion can be clone both direction, forward and backward. All that require is to exchange the position of the input and output data for the regression program. Because the polynomial coefficients are obtained by a global least square error minimization, the polynomial may not map the sample points to their original values. Several recent publications use this technique for color scanner and printer characterizations and calibrations. The adequacy of the method depends on the relationship between the source and destination spaces, the number and location of the points chosen for the regression, the number of terms in the polynomial, and the measurement error. For nonlinear color space conversion, this regression method does not guarantee uniform accuracy across the entire color gamut. In general, the accuracy improves as the number of terms in the equation increases. The trade-off is the higher computation cost and lower processing speed.[9]

*2.1.4 3D-interpolation*

The three-dimensional (3D) look-up table with interpolation is a relatively new development in color space transformation. It consists of three parts: packing (or partition), extraction (or find), and interpolation (or computation). Packing is a process that divides the domain of the source space and populates it with sample points to build the look-up table. In general, the table is built by an equal-step sampling along each axis of the source space. This will give $(n-1)^3$ cubes and $n^3$ lattice points where $n$ is the number of levels. The advantage of this arrangement is that it implicitly supplies the information about which cell is next to which. Thus, one needs only to store the starting point and the spacing for each axis. Generally, a matrix of $n^3$ color patches at the lattice points of the source space is made, and the destination color specifications of these patches are measured. The corresponding values from the source and destination spaces are tabulated into a look-up table. Non-lattice points are interpolated by using the nearest lattice points. This is the step where the extraction performs a search to select the lattice points necessary for computing the destination specification of the input point. A well-packed space can make the search simpler. In an 8-bit integer environment, for example, if the axis is divided into $2^j$ equal sections where $j$ is an integer smaller than 8, then the nearest lattice points are given in the most significant $j$ bits, $(MSB_j)$, of the input color signals. In other words, the input point is bounded in between the lattice points of $p(MSB_j)$ and $p(MSB_j+1)$. This involves the computer operations of masking and shifting bits, which are faster than the comparison operation. For non-equally spaced packing, a series of comparisons will be needed to locate the nearest lattice points. Further

selection within the cubic lattice points is required. Depending on the interpolation technique employed to compute the color values of non-lattice points, we have the geometrical method and cellular regression.

There are four geometrical interpolations: trilinear, prism, pyramid, tetrahedral and many variations. All geometric interpolations except the trilinear approach require a search mechanism to find the subdivided structure where the point resides. *[10]*

## 2.2   Literature Reviews

### 2.2.1 High Precision Color Masking in Sub-divided CIELAB Polar Coordinates Spaces

The higher precision color approximation has been approached by the optimization in sub-divided color spaces. The input color space is divided to four models: Tri-linear, LAB vector, LC, and Polar coordinates. The 1st, 2nd, and 3rd order of linear regression model applied to each sub-divided color spaces. Then, the result compared by means of color difference in *CIELAB* space.

Non-uniform division to sub-spaces, including the equal number of color samples in each, makes it possible to use the higher order of color masking and resulted in high precision reproductions with color difference in *CIELAB* space $\Delta E_{ab}*$ *(rms)*$\leq 2$ for inkjet printer. As compared with conventional color transforms by single matrix, the color errors in the proposed methods could be reduced to two third or less inside the device gamut.

The Tri-linear division gives the best result on $2^{nd}$ order linear regression model while root mean squares, *rms*, color difference is increased for $3^{rd}$ order. The reason may be caused by the unevenness of color sample numbers in each sub-space. And, in the uniform divisions, the sufficient sample numbers can't be guaranteed enough to derive the higher order coefficients when the number of sub-divisions increases.

Polar coordinates division in the hue angle and radial directions, is considered to be more stable in both trained and non-trained estimations, because the sub-space surrounded by $\Delta\theta_i$ and $\Delta r_k$ will include the color samples resemble in hue and colorfulness and the spherical boundary can cover the printer gamut more reasonably. It resulted in $\Delta E_{ab}*(rms) \leq 2.4$ for trained targets and $\Delta E_{ab}*(rms) \leq 2.2$ for non-trained target with $3^{rd}$ order.

LAB vector division with $3^{rd}$ order masking resulted in the highest reproduction with $\Delta E_{ab}*(rms) \leq 1.5$ for trained targets, and LC division with $3^{rd}$ order masking resulted in the highest reproduction with $\Delta E_{ab}*(rms) \leq 2.1$ for non-trained targets. These values are almost approaching to the mechanical stability about $\Delta E_{ab}*$ $(rms) \leq 1.0$ in inkjet printer.[11]

*2.2.2 Representtation of Color Space Transformations for Effective*

*Calibration and Control*

The *Minvar* algorithm is an application of the combination of regression model which applied to sub-space. The smallest sub-space is based on four knot in

domain space, which is called *Simplex*. The algorithm use combination of this simplex to form a larger sub-space. The size of the combination is freedom.

Each iteration of the *Minvar* algorithm consists of two basic steps. In the first step, for each simplex in the domain triangulation, the least squares linear fit is computed for the data in that cell. These are locally optimal, but in general will be discontinuous at the simplex boundaries. The least squares linear fit can be computed in closed form.

The second step in the *Minvar* algorithm moves the knots of the *Piecewise Linear (PL)* function to enforce continuity while trying to match the least squares fits. In the *GI* algorithm, this step moves the knot point to the intersection of the least squares fits from knot's two neighboring cells.

It is instructive to compare the errors of these approximations in relation to the number of parameters each approximation has its disposal. The result shown in Figure 2-2.*[12]*

| | Parameters | RMSE | $\Delta E$ | $L_\infty$ |
|---|---|---|---|---|
| PL ( 8,0,0,1) | 30 | 5.01 | 4.19 | 16.98 |
| PL (26,0,0,8) | 126 | 2.95 | 2.46 | 10.59 |
| PL (28,0,0,8) | 132 | 2.72 | 2.31 | 8.42 |
| PL (28,0,0,9) | 138 | 2.73 | 2.32 | 8.87 |
| PL (23,4,2,8) | 143 | 2.36 | 2.07 | 6.89 |
| LUT 3x3x3 | 81 | 6.94 | 6.17 | 16.92 |
| LUT 6x6x6 | 648 | 1.31 | 1.10 | 3.66 |
| LUT 11x11x11 | 3993 | 0.62 | 0.40 | 2.35 |

**Figure 2-2** Comparison of the *Minvar* algorithm to Tetrahedral interpolation